Supplementary Information

Erythrocyte Membrane-Enveloped Molybdenum Disulfide Nanodots for Biofilm Elimination on Implants via Toxin Neutralization and Immune Modulation

Tingwang Shi,[a,1] Zesong Ruan,[a,1] Xin Wang,[a] Xiaofeng Lian [a,*] Yunfeng Chen[a,*]

[a] Department of Orthopedic Surgery, and Shanghai Institute of Microsurgery on Extremities, Shanghai Jiao Tong University Affiliated Sixth People's Hospital, Shanghai 200233, P. R. China

[1] These authors contribute equally to this work.

*E-mail addresses: xf909@126.com, chenyf@sjtu.edu.cn

Additional details on experimental section

1. Materials

Ammonium tetrathiomolybdate ($(NH_4)_2MoS_4$), polyvinylpyrrolidone (PVP, M_w: 10 kDa), and hydrazine hydrate were purchased from the Shanghai Aladdin Bio-Chem technology Co., LTD (Shanghai, China). The BCA kit, 3,3′,5,5′-Tetramethylbenzidine (TMB), TMB stopping buffer, DAPI, crystal violet solution, Triton-X-100 solution, bovine serum albumin (BSA), 5(6)-Carboxyfluorescein diacetate succinimidyl ester (CFDA-SE), and 2',7'-Dichlorodihydrofluorescein diacetate (DCFH-DA) were purchased from Beyotime Biotechnology (Shanghai, China). Polycarbonate membranes (100, 200, and 400 nm) were purchased from Avanti Polar Lipids, Inc (Alabaster, AL, USA). The CCK-8 reagent was purchased from Dojindo Molecular Technologies (Kumamoto, Japan). α-hemolysin derived from *staphylococcus aureus*,

rabbit anti-Staphylococcal α-toxin polyclonal antibody were purchased from Merck (Darmstadt, Germany). 4% paraformaldehyde was purchased from Wuhan Servicebio Technology Co., (Wuhan, China). Rhodamine-labeled phalloidin was purchased from Yeasen Biotechnology (Shanghai) Co., Ltd. (Shanghai, China). Tryptone soy broth was purchased from Solarbio Science & Technology Co., Ltd. (Beijing, China). LIVE/DEAD BacLight Bacterial Viability Kit, CellTraker Red CMTPX dyes were purchased from Thermo Fisher Scientific (Waltham, MA, USA). Rabbit anti-mouse CD197 monoclonal antibody, Rabbit anti-mouse iNOS monoclonal antibody, rabbit anti-mouse Arg-1 polyclonal antibody, rat anti-mouse CD86 monoclonal antibody, Alexa Fluor 594 labeled goat anti-rabbit polyclonal antibody, Alexa Fluor 594 labeled goat anti-rat polyclonal antibody, and Alexa Fluor 488 labeled goat anti-rabbit polyclonal antibody were purchased from Abcam (Cambridge, UK). APC-labeled CD86 monoclonal antibody, PE-labeled CD206 monoclonal antibody were purchased from BioLegend (San Diego, CA, USA). Moreover, ELISA kits (TNF-α, IL-1β, MCP-1, IL-10) were purchased from Anogen (Mississauga, Canada). The RNA Purification Kit, Color Reverse Transcription Kit, 2ᵡColor SYBR Green qPCR Master Mix were purchased from EZBionscience (Roseville, USA). Primers (TNF-α, IL-1β, MCP-1, and IL-10) were purchased from BioTNT (Shanghai, China). The TRIzol reagent was purchased from TaKaRa (Kusatsu, Japan).

2. Cell lines and bacteria

We purchased RAW 264.7 and L-929 cell lines from the Cell Bank of Type Culture Collection of Chinese Academy of Sciences. Methicillin-resistant *Staphylococcus aureus* (MRSA; ATCC43300) was provided by the Department of Clinical Laboratory of Shanghai Jiaotong University affiliated Sixth People's Hospital.

3. Extraction of erythrocyte membrane fragments

Erythrocyte membrane fragments (EMFs) were harvested and purified according to previously established protocols[1]. In brief, 2 mL of whole blood was drawn from male Balb/c mice (7-8 weeks) by cardiac puncture using a heparin-containing syringe. After centrifugation (800 g, 5 min, 4 ℃), the whole blood was layered and its upper layers including plasma and buffy coat were discarded. Thereafter, erythrocytes were washed

with icy heparin-containing 1 × PBS for three times, following which they were hemolyzed in a hypotonic solution (0.25 × PBS) in ice bath for 30 min. Subsequently, the mixture was centrifuged at 20000 g for 10 min to collect lower pink pellet. Next, the pellet was washed and further centrifuged thrice to harvest purified EMFs. Finally, the resulting EMFs were resuspended in PBS and stored at -80 ℃ for further use. Meanwhile, a BCA kit was employed to determine the protein contents of EMFs.

4. Characterization of EM@MoS_2

Transmission electron microscopy (TEM) images of MoS_2 and EM@MoS_2 were recorded on a JEM-2100F field emission TEM (JEOL, Ltd., Tokyo, Japan). The physical form and chemical composition of MoS_2 NDs was measured by X-ray photoelectron spectroscopy (XPS, ESCALAB 250Xi, Thermo Fisher, Waltham, MA, USA). Ultraviolet-visible-near-infrared (UV-vis-NIR) spectra were recorded using a Lambda 750 spectrometer (PerkinElmer, USA). The hydrodynamic particle size and zeta potentials of MoS_2 NDs and EM@MoS_2 were determined using a Malvern zetasizer Nano ZS unit (Nano ZS90, Malvern Panalytical, UK). To compare the protein profiles of EM@MoS_2 nanocomposite with that of EMFs, sodium dodecyl sulfate-polyacrylamide gel electrophoresis (SDS-PAGE) was employed to isolate and further identify their protein component as previously reported[2].

5. Photothermal effect of MoS_2 NDs and EM@MoS_2

MoS_2 NDs (200 mg/L, 500 μL), EM@MoS_2 (200 mg/L, 500 μL) or EMFs (with 200 mg/L membrane protein, 500 μL) were exposed to 808 nm NIR irradiation (1 W/cm^2, 10min), respectively, and their temperature-time curves were recorded using an infrared thermal imager (Fotric 220, ZXF, USA). Then their temperature changes from the beginning to the end of irradiation were calculated, respectively. To test the photothermal-conversion performance of EM@MoS_2 at different concentrations (0, 25, 50, 100, and 200 mg/L), corresponding temperature profiles under NIR irradiation (1 W/cm^2, 10min) were recorded. Similarly, the temperature profiles under different laser power density (0.6, 0.8, 1.0, 1.2 W/cm^2) were also recorded. Furthermore, the photostability of EM@MoS2 at 200 mg/L was examined for four repeated cycles of laser on/off.

6. Peroxidase activity of EM@MoS_2

The ability of EM@MoS_2 to catalyze the decomposition of H_2O_2 was evaluated using 3, 3',5, 5'-tetramethylbenzidine (TMB) as the substrate (10 mg/mL). Firstly, EM@MoS_2 (200 mg/L) and TMB were added to NaAc buffer (pH = 4.5) containing a series of concentrations of H_2O_2 (5 mM, 10 mM, 15 mM, and 20mM). After incubation for 5 min, the absorbance of oxidized TMB (ox-TMB) at 635 nm was recorded using UV-vis spectra (Shimadzu, Tokyo, Japan). Subsequently, the catalyzing reactions under various concentrations (0, 25, 50, 100, and 200 mg/L) of the EM@MoS_2 or different buffer pH (3.0, 4.5, 6.0, and 7.5) were also monitored as descried above. The ESR was performed under different pH values with 5,5-dimethyl-1-pyrroline N-oxide (DMPO) as the spin trap on JEOL FA200 electron paramagnetic resonance spectrometer. The kinetic parameters including Michaelis constant (K_m) and maximum reaction velocity (V_{max}) were determined by nonlinear regression analysis based on Michaelis-Menten equation:

$$v = \frac{V_{max}[S]}{K_m + [S]}$$

where v represents the initial velocity, [S] refers to the concentration of substrate. In addition, we evaluated the catalytic activity of EM@MoS_2 with the concentration of TMB or H_2O_2 varied, and the other being fixed. Subsequently, the obtained data were fitted into the double reciprocal Lineweaver-Burk plots.

7. Biocompatibility of MoS_2 NDs and EM@MoS_2

A standard CCK-8 assay was conducted on RAW 264.7 cells to evaluate the biocompatibility of MoS_2 NDs and EM@MoS_2. Briefly, RAW 264.7 cells were seeded in 24-well plate at a density of 5×10^4 cells per well and incubated under standard condition (37 ℃, 5% CO_2) overnight. Then cells were treated with a series of graded concentrations of MoS_2 NDs or EM@MoS_2 (0, 25, 50, 100, 200, and 400 mg/L) for 24 h. Finally, the relative cell viabilities were detected using CCK-8 reagent according to specifications. The experiment was repeated three times under the same conditions.

8. In vitro antibiofilm effect and mechanisms

The MRSA strain ATCC43300 was used to cultivate bacterial biofilms. The

antibiofilm effects of MoS_2 NDs and EM@MoS_2 were evaluated in five experimental groups: control, NIR (808 nm, 1.0 W/cm^2, 10 min), MoS_2, EM@MoS_2, and EM@MoS_2 + NIR laser (808 nm, 1.0 W/cm^2, 10 min). In addition, polyether-ether-ketone (PEEK) small discs (10 mm in diameter and 0.5 mm in thickness) were chosen as the substances to culture biofilms. The peek tablets were pre-sterilized by 50kGy electron beam irradiation for 1 min. To cultivate MRSA biofilm, 500 μL of bacteria suspension (10^6 CFU/mL) was added onto the PEEK disc placed in 24-well plates and then incubated at 37 ℃ for 24 h. After that, the tryptone soy broth in each well was replaced with pure PBS (control and NIR groups) or nanomaterial solutions [MoS_2 NDs or EM@MoS_2 (200 mg/L)], and all samples were incubated for another 6 hours at 37 ℃. Specially, NIR and EM@MoS_2 + NIR groups were irradiated under 808 nm NIR for 10min. Finally, the small discs in each group were rinsed three times for the following experiments.

For standard plate counting tests, samples of each group were transferred into EP tubes containing 1mL PBS under aseptic conditions. Then the bacterial suspensions were collected by rapid vibration, subsequent sonication, and 10-fold gradient dilution. Next, 100 μL suspension of each diluted gradient of each sample was used to coat blood agar plates. After all the plates were incubated overnight in 37 °C, bacterial colonies were counted. For crystal violet staining, the treated PEEK discs were firstly fixed with 99% methanol for 15 min, and then stained with 2% crystal violet solution for 5 minutes. To visually monitor the residual crystal violet (equivalent to remaining biomass of biofilms), all the samples were fully rinsed and dried before photographed. Meanwhile, quantitative analysis was performed by dissolving remaining crystal violet with 33% acetic acid and detecting the absorbance of resultant eluent at 550 nm by an Epoch-2 microplate reader (BioTek Instruments, Winooski, VT, USA).

9. Cell culture and intervention for the assessment of Immunoregulatory potential

RAW264.7 cells were seeded in 6-well plates or confocal dishes (for immunofluorescence staining) at a density of 2×10^5 cells per well (1×10^5 cells per dish), and cultured for 12 h. Afterwards, MoS_2 NDs were added to each well or dish and the final concentrations were adjusted to 25, 50, 100, and 200 mg/L, respectively.

Meanwhile, 200 mg/L of EM@MoS_2 was used to stimulate RAW 264.7 cells as well. After 24 h incubation, the nanomaterial-containing medium was removed and cells were rinsed for subsequent trails. The PBS-treated group was considered as the control.

10. Immuno-antibiofilm therapy mediated by EM@MoS_2

In order to visually explore the potency of EM@MoS_2-pretreated macrophages to penetrate biofilms and phagocytose bacteria, CellTraker Red CMTPX dyes and CFDA-SE were selected to label living macrophages and living bacteria, respectively.

To obtain activated macrophages (AM), RAW 264.7 cells were pretreated with EM@MoS_2 (200 mg/L) as described above. Meanwhile, the cells treated with PBS were considered as unactivated macrophages (UM). After stained with CellTracker Red CMTPX dye working solution (5 μM) for 20 min, AM and UM were gently scraped and washed for subsequent usage. At the same time, MRSA biofilms without any treatment were set as intact biofilms (IB), whereas biofilms pretreated with EM@MoS_2 + NIR were grouped as cracked biofilms (CB). Then, IB and CB were labeled with CFDA-SE (5 μM) in a dark room for 30 minutes, following which excess dyes were removed. Thereafter, 3×10^5 red fluorescence-labeled AM or UM were added onto the green fluorescence-labeled biofilms and incubated at 37 °C for two hours. Eventually, the interaction between macrophages and biofilms was observed and imaged by CLSM. Additionally, we evaluated the difference between the groups by counting the number of cells penetrating the biofilms.

Furthermore, the phagocytic potency and bactericidal abilities of AM and UM were investigated. In this part of the experiment, CB were collected from IB by vibration and sonication and further stained with CFDA-SE. Subsequently, stained IB suspension (100 μL, 1×10^7 CFU/ml) and CellTracker Red-labeled AM or UM suspensions (1mL, 1×10^5/mL) were mixed and cocultured in confocal dishes for 2 h. Afterwards, the cells were gently scraped and centrifuged (1500 rpm, 5 min) to remove the bacteria that had not been phagocytosed. Later, cell samples were cultured in new confocal dishes for 30 min until attachment for subsequent CLSM observation. Moreover, to quantitatively explore the bactericidal potency of AM, biofilm fragments (100 μL, 1×10^7 CFU/mL) and AM or UM suspension (1 mL, 1×10^5/mL) were mixed and cocultured for 3 h.

Afterwards, mixed suspensions were used for plate counting tests and bacterial viabilities was determined in each group.

Supplementary Tables and Figures

Table S1. Primers used in the RT-PCR experiment.

Gene	Upper primer sequence (5' to 3')	Lower primer sequence (5' to 3')
TNF-α	TAGCCAGGAGGGAGAACAGA	CCAGTGAGTGAAAGGGACAGA
IL-1β	TACATCAGCACCTCACAAGC	AGAAACAGTCCAGCCCATACT
MCP-1	CATCCACTACCTTTTCCACAA	CATCACAGTCCGAGTCACAC
IL-10	AGTGTGTATTGAGTCTGCTGG	GAGAGAGGTACAAACGAGGTT
GAPDH	AAATGGTGAAGGTCGGTGTG	AGGTCAATGAAGGGGTCGTT

Table S2. The K_m and V_{max} of different nanozymes with H_2O_2 as the substrate.

Nanozyme	K_m (mM)	V_{max} (10^8 M s^{-1})	Reference
MoS_2 NDs	1.94	12.76	this work
MoS_2 nanoflowers	2.81	8.01	3
horseradish peroxidase	3.70	8.71	4
Fe_2O_3	86.43	3.05	5

Table S3. The detailed calculation process of the exact toxin adsorption amount of EM@MoS_2 according to BCA assay.

Group	Absorbance	EM@MoS_2	Total	Non-adsorbed	Adsorbed	Averag

s	at 562 nm	(mg)	toxins (μg)	toxins (μg)	toxins (μg)	e (μg)
1	0.312	1	120	42	78	
2	0.377	1	160	78.5	81.5	78.83
3	0.528	1	240	163	77	

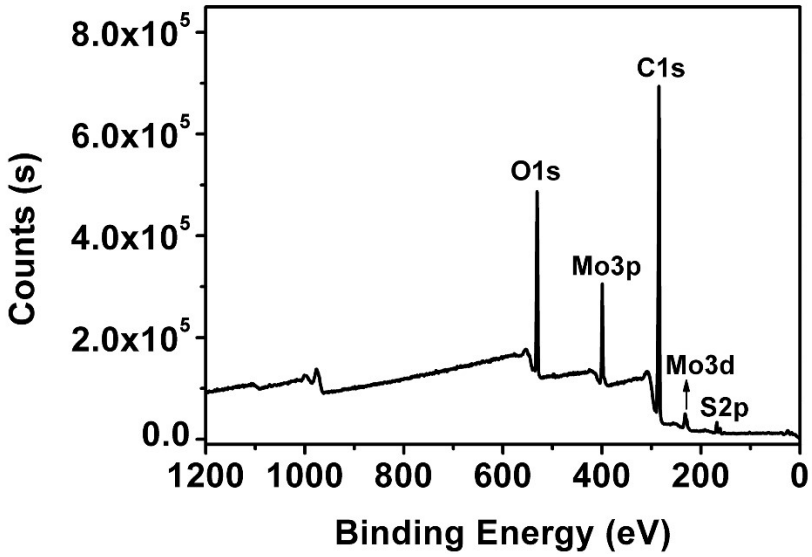

Fig. S1. The XPS survey spectrum of MoS_2 NDs.

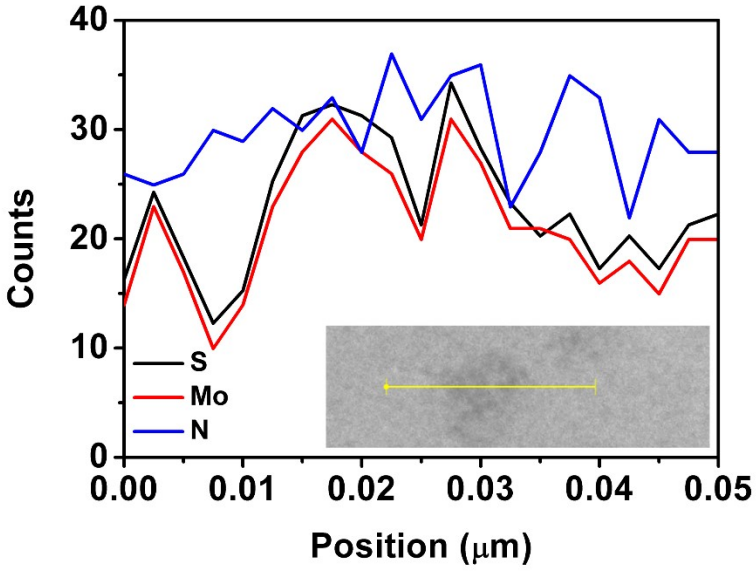

Fig. S2. Line-scan TEM-EDS elemental distribution curves of PVP-modified MoS_2 NDs along the yellow line in inset TEM image.

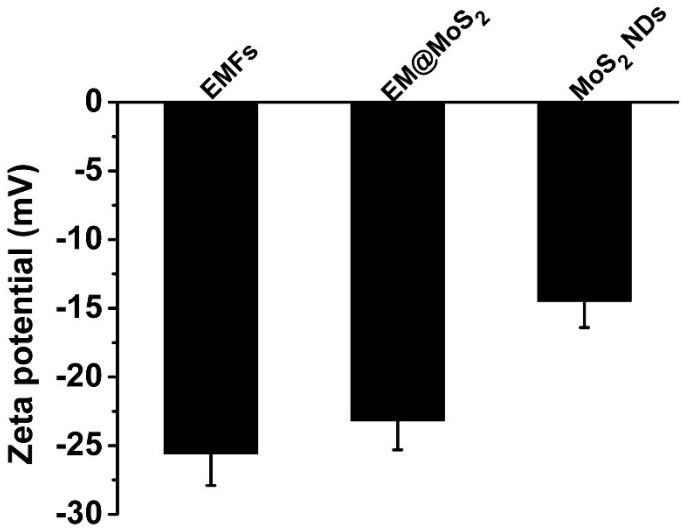

Fig. S3. Zeta potentials of EMFs, MoS_2 NDs, and EM@MoS_2 dispersions in DI water.

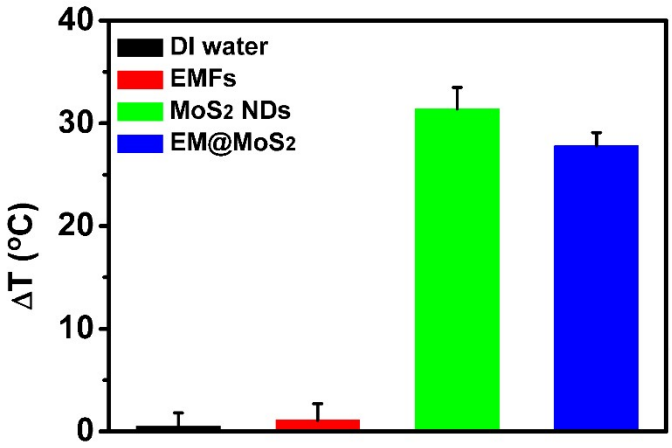

Fig. S4. Temperature changes of EMFs, MoS_2 NDs, and EM@MoS_2 dispersions under irradiation of 808 nm laser at the power density of 1.0 W cm^{-2} for 10 min.

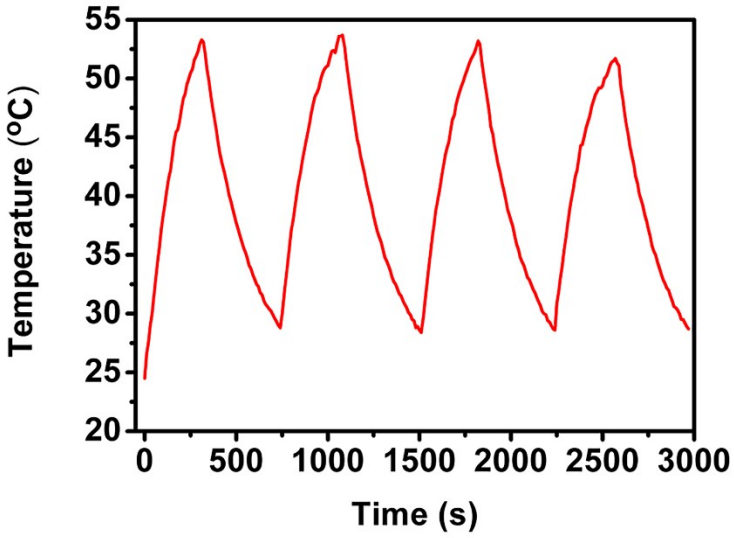

Fig. S5. The temperature-time curve for EM@MoS_2 dispersion during four laser on/off cycles.

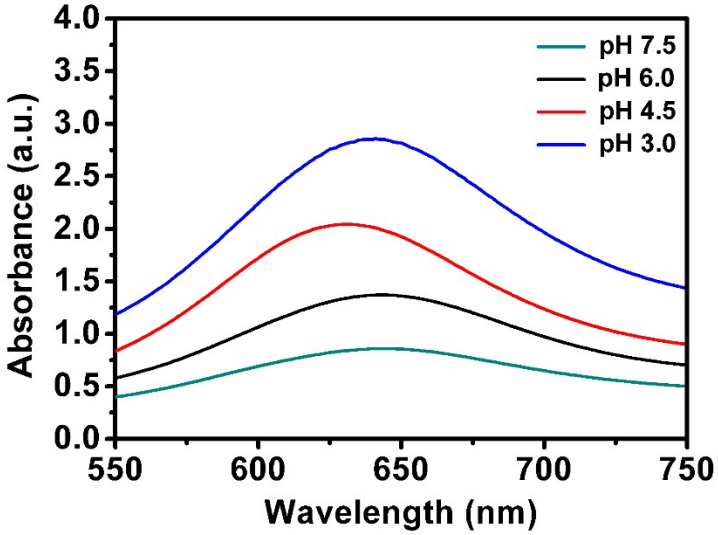

Fig. S6. UV-vis absorbance spectra of ox-TMB in the presence of H_2O_2 and EM@MoS_2 at different pH values.

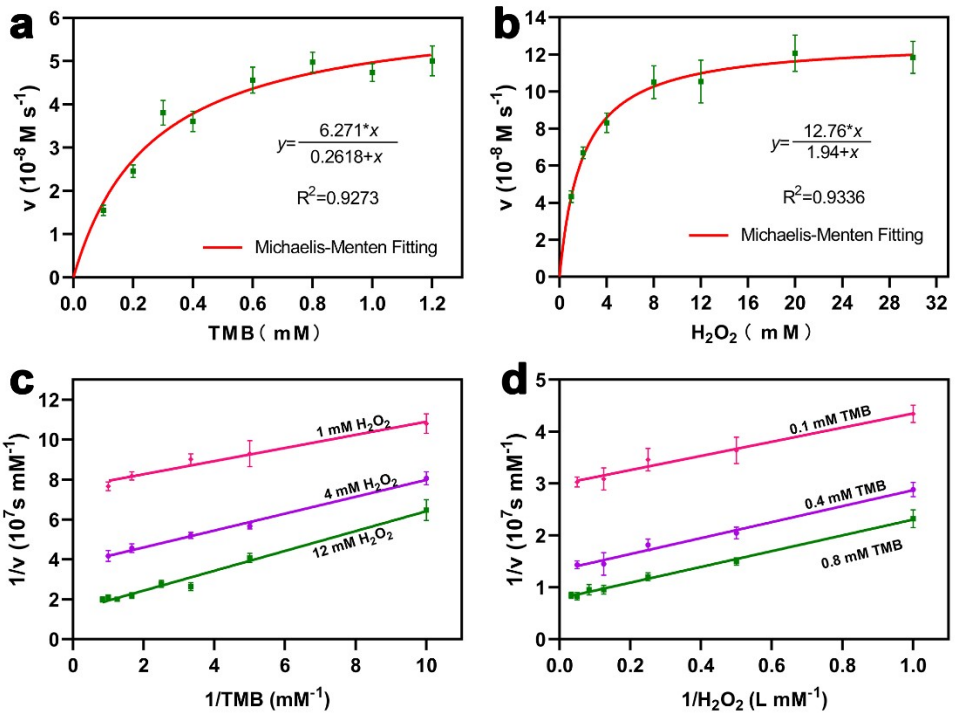

Fig. S7. Steady-state kinetics analysis of EM@MoS_2. (a) Michaelis–Menten kinetics of EM@MoS_2 under fixed H_2O_2 concentration (12 mM) and varied TMB concentrations. (b) Michaelis–Menten kinetics of EM@MoS_2 under fixed TMB concentration and varied H_2O_2 concentrations. Lineweaver–Burk plotting of EM@MoS_2 with the concentration of H_2O_2 (c) or TMB (d) fixed and the other varied. The error bars indicate the standard deviation (n = 3).

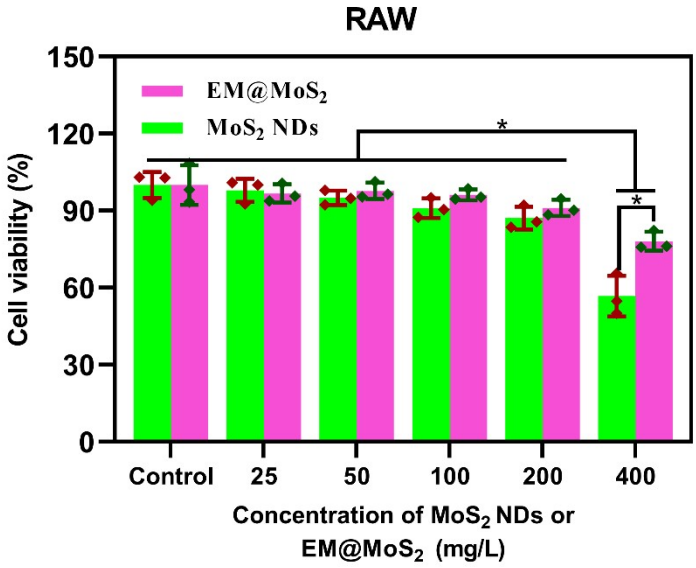

Fig. S8. Cell viability of RAW 264.7 cells measured by CCK8 assay after treated by different concentrations of MoS_2 NDs or EM@MoS_2 for 24 h. Note: * ($p < 0.05$).

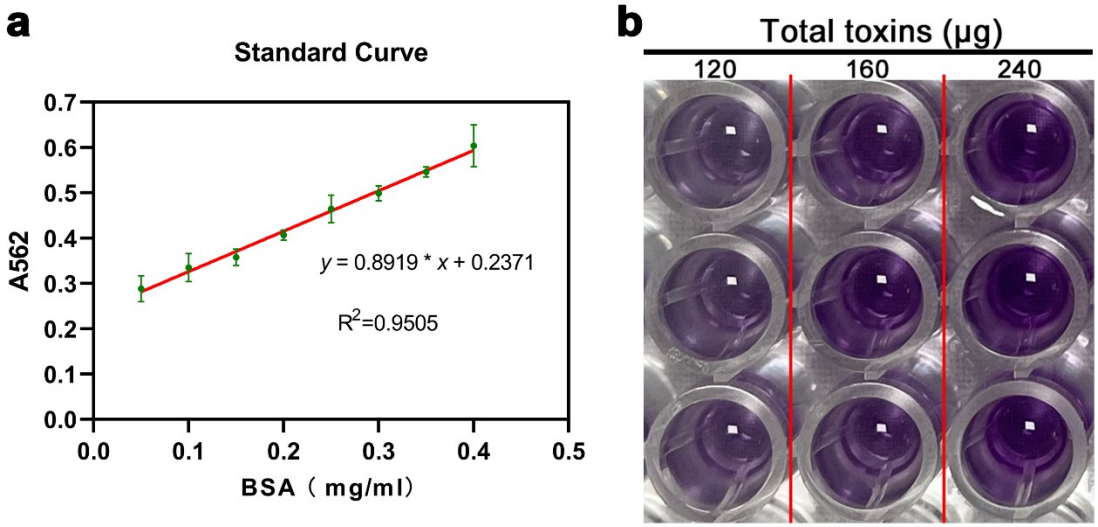

Fig. S9. Detection of non-adsorbed toxins after incubation with EM@MoS_2 (500 μL, 2 mg/mL) using BCA assay. (a) The bovine serum albumin (BSA) standard curve plotted according to a BCA kit. (b) The chromogenic reaction between non-adsorbed toxins and BCA working solution after co-incubation for 30 min.

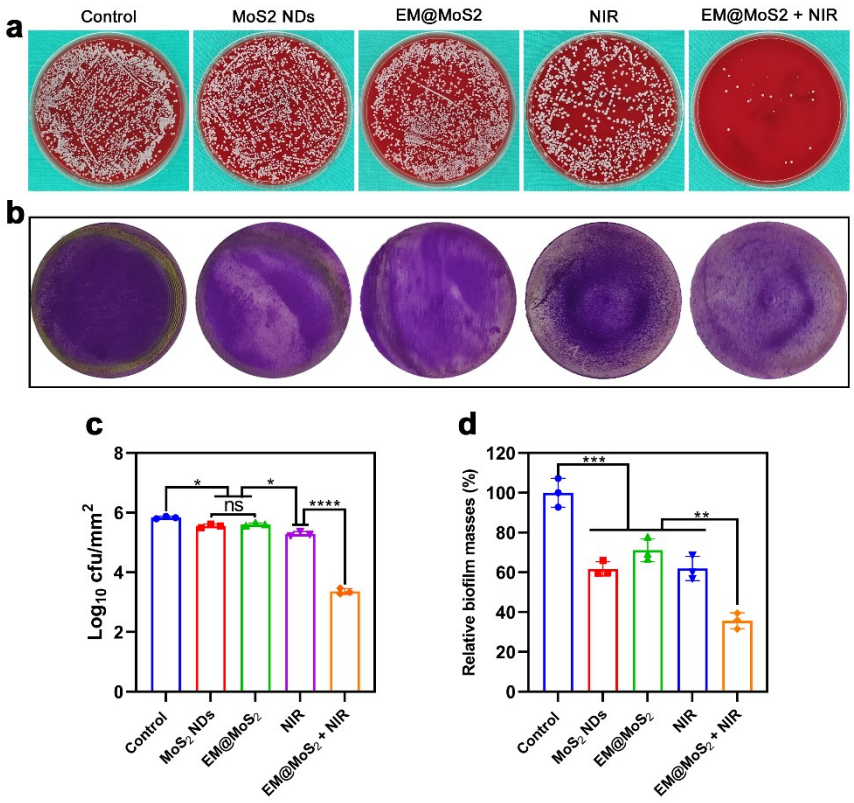

Fig. S10. In vitro antibiofilm effect of MoS_2 NDs and EM@MoS_2. (a) Representative images of bacterial colonies from different groups. (b) Crystal violet staining images of residual biofilms after different treatments. (c) Quantitative analysis of bacterial colonies from different groups using standard plate counting tests. (d) Quantitative analysis of residual biofilm masses. Note: * ($p < 0.05$), ** ($p < 0.01$), *** ($p < 0.001$), **** ($p < 0.0001$).

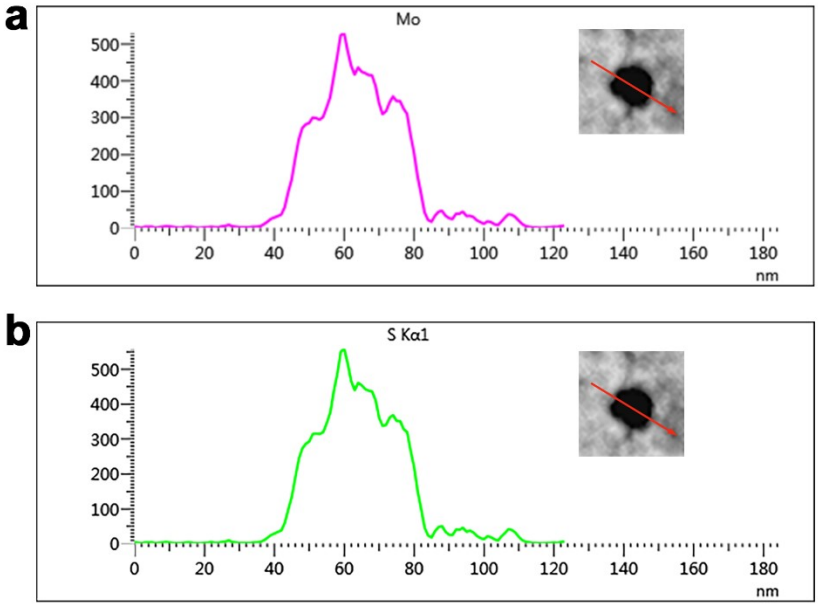

Fig. S11. EDX line scan analysis along the red line in inset TEM image.

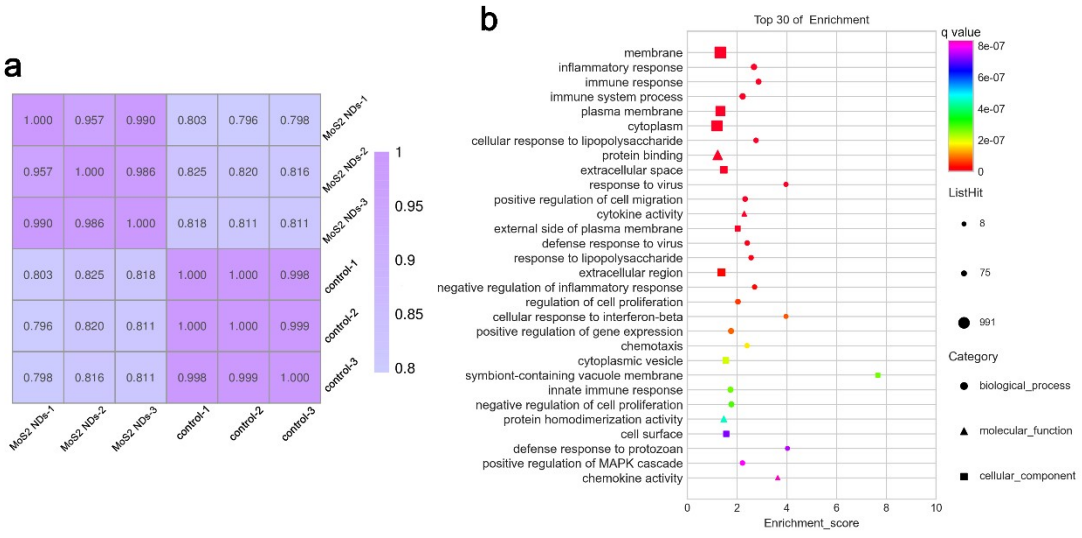

Figure. S12. RNA-seq analysis of RAW 264.7 gene expression. (a) Heatmap of correlation analysis between samples. (b) GO analysis of differential expressed genes.

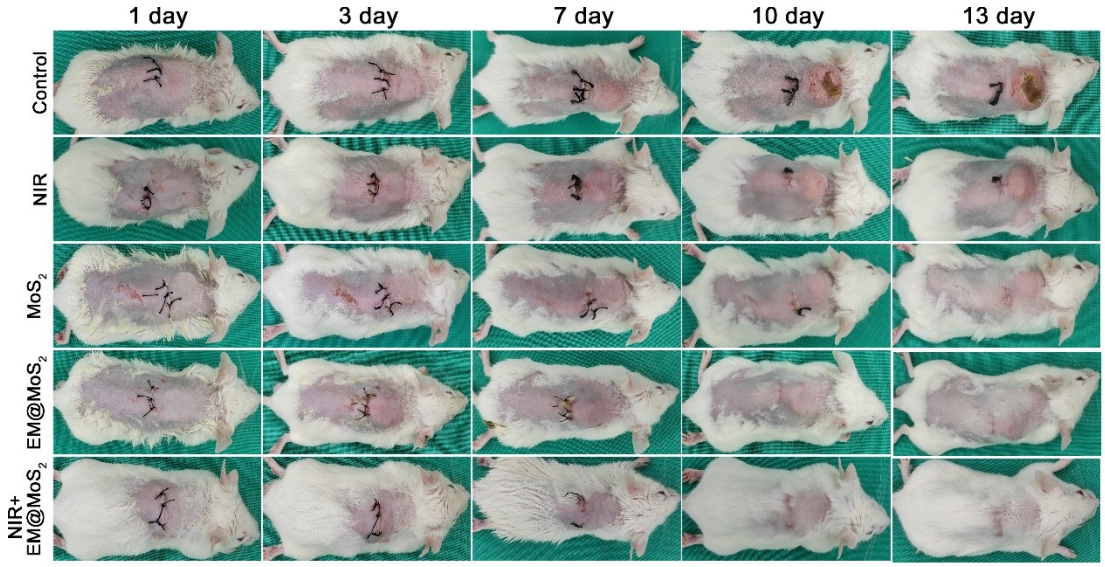

Figure. S13. Typical photos of mouse subcutaneous implant-related infection models after different treatments over the course of thirteen-day observation.

Figure. S14. General observation of implants together with peri-implant soft tissues incised from infection area.

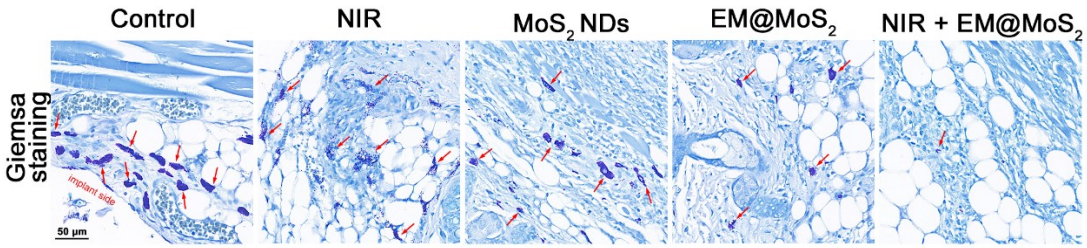

Figure S15. Giemsa staining image showing residual biofilms in peri-implant soft tissues.

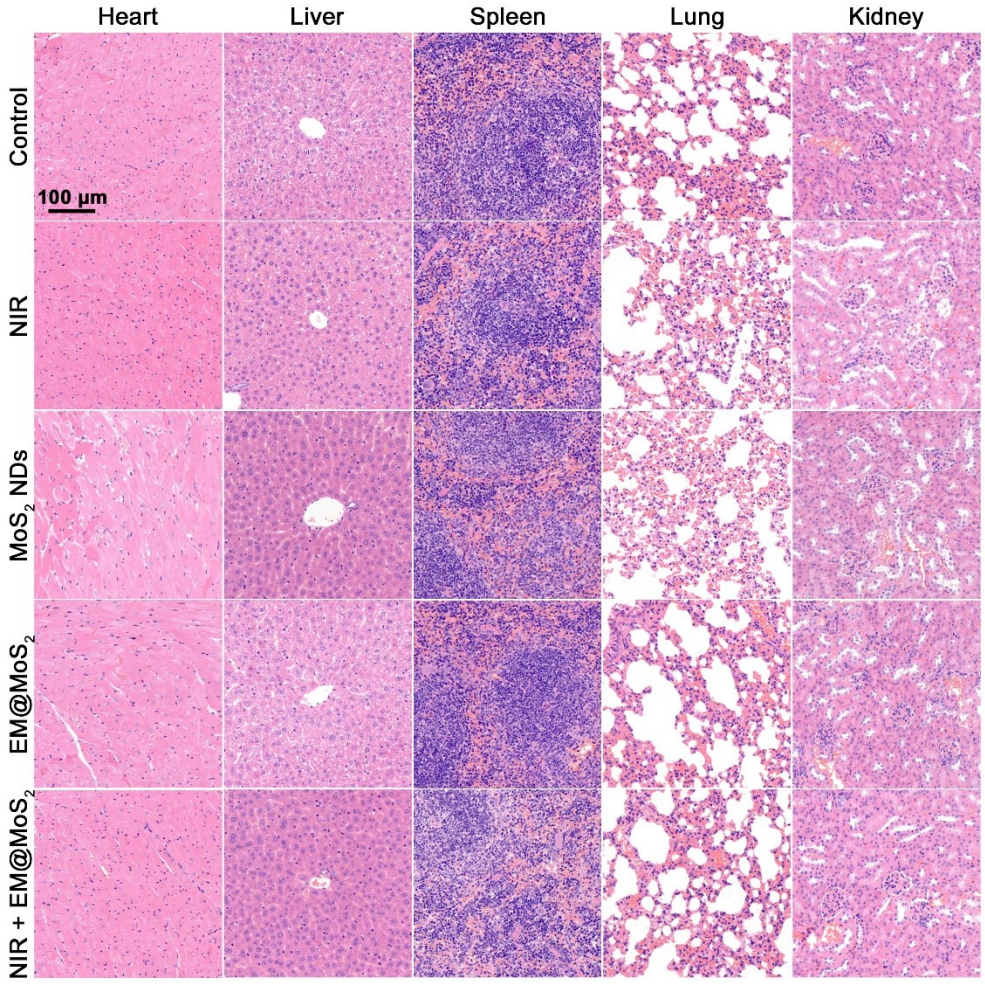

Figure. S16. Images of H&E-stained sections of major organs (heart, liver, spleen, lung and kidney) after different treatments.

Supplementary References

1 Q. Jiang, Y. Liu, R. Guo, X. Yao, S. Sung, Z. Pang and W. Yang, *Biomaterials*, 2019, **192**, 292–308.

2 C.-M. J. Hu, L. Zhang, S. Aryal, C. Cheung, R. H. Fang and L. Zhang, *Proc. Natl. Acad. Sci. U. S. A.*, 2011, **108**, 10980–10985.

3 W. Yin, J. Yu, F. Lv, L. Yan, L. R. Zheng, Z. Gu and Y. Zhao, *ACS Nano*, 2016, **10**, 11000–11011.

4 L. Gao, J. Zhuang, L. Nie, J. Zhang, Y. Zhang, N. Gu, T. Wang, J. Feng, D. Yang, S. Perrett and X. Yan, *Nat. Nanotechnol.*, 2007, **2**, 577–583.

5 S. Tanaka, Y. V. Kaneti, R. Bhattacharjee, M. N. Islam, R. Nakahata, N. Abdullah, S.-I. Yusa, N.-T. Nguyen, M. J. A. Shiddiky, Y. Yamauchi and M. S. A. Hossain, *ACS Appl. Mater. Interfaces*, 2018, **10**, 1039–1049.